LABORATORY UWB GPR SYSTEM FOR LANDMINE DETECTION

B. Scheers, Y. Plasman, M. Piette, M. Acheroy
ELTE Dep., Royal Military Academy
30, Avenue de la Renaissance B-1000 Brussels
bart.scheers@elec.rma.ac.be, marc.piette@tele.rma.ac.be, marc.acheroy@elec.rma.ac.be

A. Vander Vorst
Hyperfréquences U.C.L., Belgium
vandervorst@emic.ucl.ac.be

ABSTRACT

In this paper, the design and the modelling of an indoor impulse UWB GPR systems (1GHz-5GHz), built in the scope of the HUDEM project, is presented. For an impulse UWB system, a time-domain modelling is an obvious choice. We explain how the antennas can be characterised by their normalised impulse response. By considering the antenna as a convolution operator, we get a mechanism for modelling the whole radar system as a cascade of linear responses, which gives a lot of advantages and possible application. In our research it is used to express the radar range equation in the time-domain, to optimise the antenna configuration and to tune signal-processing algorithms. The deconvolution of the signal source and antenna impulse responses is an ill posed operation. In this paper we present a method for decomposing an A-scan in a linear combination of wavelets, using the Continuous Wavelet Transformations - by properly choosing the mother wavelet. This technique can also be used to reduce the amount of data for further processing. Finally, results obtained by our UWB GPR system are shown. Advantages and shortcomings are discussed.

INTRODUCTION

The Ground Penetrating Radar is a promising technology for detection and identification of buried landmines. Conventional GPRs usually work at central frequencies below 1GHz (Daniels, 1996). As landmines are small objects and often shallow laid, a large bandwidth is needed for a better depth resolution and detailed echo. The use of impulse wideband systems involves some technical problems. Critical points are the UWB antennas.

In our research on the detection and classification of plastic AP mines by means of UWB GPR, we built an indoor time-domain UWB GPR systems (1GHz-5GHz), to study the advantages and shortcomings of such a system. The system components are, except for the antennas, mainly off-the-shelf equipment. It consists of the following parts: on the transmitting side a Picosecond Pulse Labs step-generator is used. The generated step has an amplitude of 10 Volts, a rise-time of 45 ps and a high waveform purity. This step is then transformed by an impulse-forming-network to an impulse with a maximal amplitude of 2.5 Volts and a FWHM of less than 100 ps. On the receiver side, a 6GHz digitising oscilloscope is used to measure the backscattered signal. The oscilloscope has an internal delay line, a 14 bit resolution and can average up to 10000 times, to obtain a higher dynamic range. The antenna pair consists of two TEM horn antennas and is mounted on a computer-controlled xy-table of 2m by 2.5m and 2m high. In the scanning area of the table, two boxes are placed, 1.5m by 1.5m each and 0.8m deep. The first one is filled with sand, the second one with loam. The permittivity of both types of soil is fully characterised in function of frequency and moisture content.

THE DIELECTRIC-FILLED TEM HORN ANTENNA

The main effort was put in the development of directive UWB TEM horn antennas (Scheers et. al, 2000a) that can be used off-ground. In the design we tried to limit the dimensions and weight of the antennas to guarantee a high degree of mobility. To reduce the physical size of the antennas and to improve the directivity, without reducing too much the bandwidth, the antennas were filled with a dielectric ($e_r \approx 3$). Antenna measurements revealed indeed that the antennas were more directive, the frequency coverage moved towards the lower frequencies compared to the air-filled antennas. The antenna plates were etched on a printed circuit board (PCB) and terminated by a 50 Ohm load, by putting two 100 Ohm SMD resistors in parallel between the antenna plate extremities. We also replaced the antenna plates by a set of 41 wires. The distance between the wires is too small to influence the antenna characteristics, but it forces the currents to be radial and it limits the surface of conducting metal. The latter is very important, when using the antennas in combination with a metal detector. The TEM horns were designed to match the

50 Ω driving cable. To avoid reflection of an unbalanced current component on the coax feedline exterior, a wideband balun was integrated. The principle of this balun is based upon an electrostatic reasoning (Rumsey, 1966). A taper in the bottom plate provides a gradual transition from an unbalanced set-up (upper antenna plate on a ground plate), towards a balanced configuration (two symmetrical antenna plates).

We can see that the dielectric-filled TEM horn antenna pair is capable of radiating and receiving very short, but still clean pulses, which is of course important for this application. The relatively small 3dB beamwidth of the antennas, 32° in the H-plane and 65° in the E-plane, and the small dimensions (12*6*12cm), makes them suitable for using off-ground in hand-held applications.

ANTENNAS AS CONVOLUTION OPERATORS

A common way of describing antennas in the time domain is by means of their impulse response (IR). Different types of IRs can be defined. We opted for the normalised impulse response (normalised IR), i.e. an impulse response integrating all frequency dependent antenna characteristics (Scheers et. al, 2000b; Farr et. al, 1998). In this way, the time domain antenna equations, expressed in terms of the normalised IR, become very simple and accurate to use. No assumption about frequency dependent terms has to be made. To simplify the expressions, we only consider antenna performance for dominant linear polarisation of the E-field. The extension to the more general case is possible. First consider the time-domain antenna equation for the transmitting antenna. The radiated field in the far field is given by:

$$E_{rad}(r,q,j,t) = \frac{1}{2p\,r\,c} h_{N,Tx}(q,j,t) \otimes \frac{\sqrt{Z_0}}{\sqrt{Z_c}} \frac{dVs(t-r/c)}{dt} \qquad (1)$$

$h_{N,Tx}(q,j,t)$ is the normalised IR of the transmitting antenna in the direction (q,j), $V_S(t)$ is the excitation voltage at the antenna feed in a 50 Ω load, Z_c the impedance of the feed cable, and Z_0 the impedance of free space. The co-ordinates origin $\vec{r} = 0$ is taken in the virtual source of the antenna, i.e. an apparent point in the antenna from which the radiated field degrades by a factor $1/r$ (Fig.2). The received voltage $V_{rec}(t)$, in a 50 Ω load, at the feed of the receiving antenna for an incoming field $E_{inc}(t)$, evaluated in the virtual source of the antenna, is calculated by:

$$V_{rec}(t) = \frac{\sqrt{Z_c}}{\sqrt{Z_0}} h_{N,Rx}(q,j,t) \otimes E_{inc}(t) \qquad (2)$$

The two time-domain antenna equations (1) and (2) are defined in such a way that $h_{N,Tx} = h_{N,Rx}$ for two identical antennas. It is seen that within the 3dB beamwidth of the antennas, the normalised IR can be expressed as $h_N(q,j,t) = k.h_N(0,0,t)$, with $h_N(0,0,t)$ the normalised IR on boresight of the antenna and k the peak voltage pattern of the antenna in the direction (q,j). Hence the antennas are completely characterised by the two latter. The normalised IR on boresight is easy to measure, using two identical antennas and a vector network analyser (Scheers et. al, 2000b). Fig. 1 shows the normalised IR on boresight of the antennas designed for the laboratory UWB GPR.

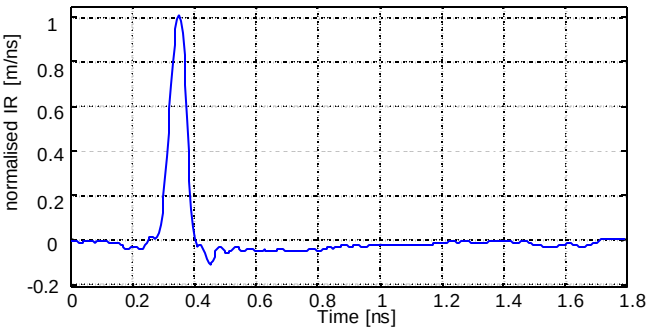

Fig.1: Normalised IR of TEM horn antenna

One of the advantages of considering the antenna as a convolution operator is that we get a mechanism for modelling the whole radar system as a cascade of linear responses.

RANGE PERFORMANCE OF THE SYSTEM

The radar range equation is a useful description of the factors influencing radar performance. Describing performances of an "impulse" system, using this equation in the frequency domain, has some drawbacks: it contains frequency dependent terms and does not specify the nature of the transmitted signal. Furthermore, it is more convenient to state the minimum detectable signal of a time-domain system as a peak voltage. Expressing the radar range equation as a cascade of impulse responses would be more practical. The backscattered field from the target, characterised by an IR $\Lambda_{v,v}(t)$, can be described as:

$$E_{scat}(r',q',j',t') = \frac{1}{4p\,r'} \Lambda_{v,v}(q',j',t') \otimes E_{rad}(t'-r'/c) \qquad (3)$$

The co-ordinate system $\vec{r}' = 0$ is connected to the target (Fig. 2). $\Lambda_{v,v}(t)$ only takes into account the backscattered

signal in the same polarisation as the incoming field and is the time equivalent of the square root of the target radar cross section.

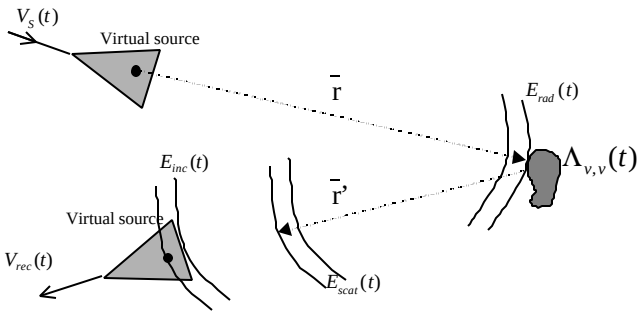

Fig. 2: Electromagnetic configuration

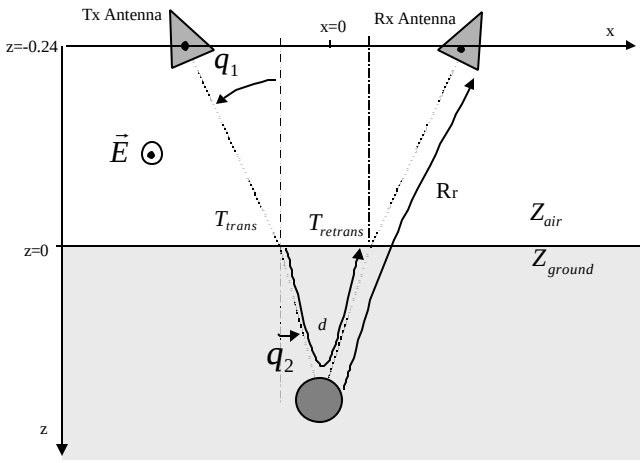

Fig. 3: Configuration of UWB GPR

Further some additional losses have to be introduced. In the scope of demining applications, using antennas off-ground, we will only take into account the transmission losses at the air-ground interface and the propagation loss in the ground. The transmission losses at the air-ground interface are given by the two oblique incident transmission coefficients T_{trans} and $T_{retrans}$ on the interface. The propagation losses in the ground are not so easy to introduce. The best way to handle with these losses is representing the ground as a low-pass filter. The transfer function of this filter, representing a propagation of *d* meters in the ground, is given by $H_d(w) = e^{-(a+jb)d}$, where α is the attenuation constant [Np/m] of the medium and β the phase constant [rad/m]. Both constants are function of frequency and complex permittivity $e' - je''$. For a given soil, i.e. texture, density and moister content, and for a given two-way path length *d* in the ground, the impulse response $g_d(t)$ of the soil, representing the propagation losses, can be calculated. Substituting equation (1), (2) and (3), and introducing the additional losses, the GPR radar range equation in the time-domain is found as:

$$V_{rec}(t) = \frac{T_{trans} \cdot T_{retrans}}{8p^2 R_t R_r c} \cdot g_d(t) \otimes h_{N,Tx}(q, j, t) \otimes \Lambda_{v,v}(t) \otimes h_{N,Rx}(q, j, t) \otimes \frac{dVs(t)}{dt} \quad (4)$$

With R_t: The total path length from transmitting antenna to the target

R_r: The total path length from receiving antenna to the target

The losses due to the off-boresight position of the target are already taken into account by $h_N(q, j, t)$.

Fig. 4 shows the range performance of our laboratory UWB system for a fictitious metallic target in a lossy rice field soil. The soil, coming from Cambodia, has a texture composition of 69% of sand, 24% of silt and 7% of clay. This sandy soil represents a regular agriculture soil with which deminers are confronted. The complex permittivity of the soil was measured in function of the moister content over a large frequency band. The target is a fictitious metallic object with an IR $\Lambda_{v,v}(t) = 0{,}314\,d(t)$, comparable to an IR of a metallic sphere with a radius of 50 mm, taking only into account the surface scattering. In the implementation, we introduced some approximations and simplifications, without loss of generality: the bistatic RCS of the target is taken independent of the bistatic angle, the antennas are always focussed on the target and the transmission coefficients suppose a flat interface, no losses in the ground and a polarisation parallel to the interface. The virtual sources of the antennas are at 24 cm above the ground and the two antennas are separated by 22.8 cm (Fig. 3). The air-ground interface is at z=0.

The minimal detectable peak amplitude of our receiver, limited by its noise performance and the antenna coupling, is about 1 mV (-47 dBm). This means that the maximal depth of the target to be detected in a 10% moister soil is 10 cm. It can be seen that the performance of an UWB system is limited by the moister content of the soil. Note that the driving source $V_S(t)$ of the laboratory system has a maximum amplitude of only 2.5 V and that the receiver has a 14 bit resolution and no time varying gain. Another impulse generator and receiver could enhance the range performance.

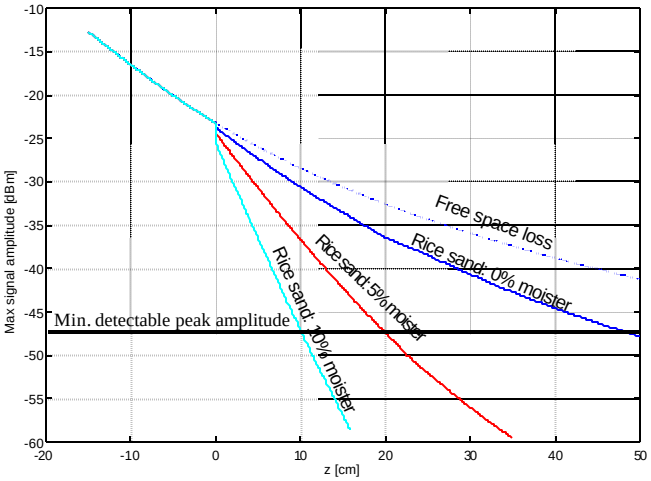

Fig. 4: Peak amplitude of the reflection on the target [dBm] in function of z [cm] for 0%, 5% and 10% moister content.

ANTENNA CONFIGURATION

In the design of the laboratory UWB GPR, a study was made to optimise the position and orientation of the Tx and Rx antennas. To reduce the coupling between the two TEM horns, they were put side by side with a common H-plane. In principle antenna coupling is not critical and can be compensated for, but if the ringing between the two antennas lasts too long, it can interfere with the useful backscattered signal. The height of the antennas above the ground is chosen to be around 25 cm.

An important parameter for the Tx-Rx antenna configuration is the combined antenna pattern – i.e. the pattern of the two antennas considered as one antenna. The resulting 3dB beamwidth of this combined antenna pattern is obviously a function of the offset angle q_1 as represented on Fig. 5a. A large 3dB beamwidth is not a priori unfavorable. When scanning over a point target with the GPR, the B-scan will show a hyperbolic structure in the reflection (Fig. 5b). A larger 3dB beamwidth produces larger hyperbolas in the B-scan, and can therefore increase the detectability of objects. As a criterion for the optimisation of this offset angle q_1, we have considered the total energy found in the hyperbolic shaped response of a point target. This total energy represents in some sense the expected reflected energy of the point target, after enhancing the B-scan by an optimal migration method. For this reason, we simulated different synthetic B-scans (Fig. 5b) of a point scatterer at 6 cm in the ground, for different values of q_1. The fictitious point scatterer is represented by a bistatic impulse response $\Lambda_{v,v} = d(t)$. For each position x of the antenna pair (Fig 5a), the backscattered signal $V_{rec}(t)$ was calculated using the radar range equation (4).

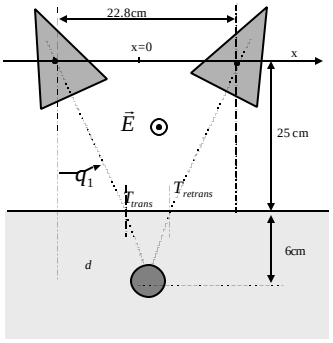

Fig. 5a: Antenna configuration

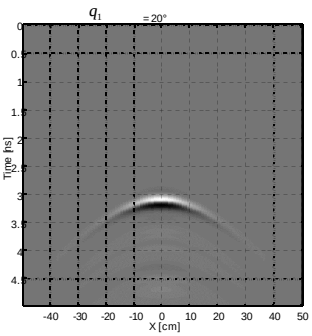

Fig. 5b: synthetic B-scan

The total energy in the hyperbolic shaped response of the target is calculated as $E_{tot} = \int_x \int_t |V_{rec}(t)|^2 dt.dx$. Fig. 6 shows the total energy in the hyperbolic response of the point target as a function of the offset angle q_1. The maximal energy in the hyperbola is found for an offset angle of 20°, which for this configuration (object at a depth of 6 cm) corresponds to the angle that focuses the antennas on the target, taking into account the refraction. In reality the depth of the object is a priori unknown, but is expected to be between 0 and 20 cm. Therefore, in the design of the laboratory UWB GPR, an angle q_1 of 20° was chosen.

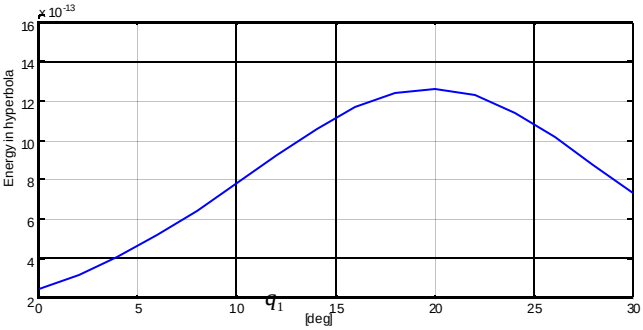

Fig. 6: Total energy in the hyperbolic shaped response of a point target at 6 cm of depth.

DECOMPOSITION OF A-SCAN IN WAVELETS

In radar applications, it is well known that the backscattering from a complex target can be approximately modelled by a discrete set of scattering centres (Trintinalia et.al, 1997). A method to extract the scattering centres of the target, and thereby enhancing depth resolution, is by deconvolving the backscattered signal. Because of the band limited nature of the emitted wave and the effect of noise, deconvolution of the backscattered signal is an ill posed

operation. An additional problem when extracting the scattering centres in GPR signal is the broadening of the reflected signal due to the dispersive behaviour of the ground.

In this section we present a method for extracting the scattering centres, that is more robust to noise and that partially compensates for the dispersive behaviour of the ground. The method, based on the Continuous Wavelet Transformation (CWT), uses the scaling properties of the wavelets to counteract the dispersive behaviour of the ground. The knowledge of the exact source signal and of the antenna IR is basic in this method.

If *k* scattering centres approximately model a scenario of complex targets and flat interfaces, the received signal can be written as a linear combination of *k* wavelets:

$$V_{rec}(t) \approx \sum_{p=1}^{k} B_p h_{a_p,t_p}(t), \qquad (5)$$

where the wavelet $h_{a_p,t_p}(t)$ models the backscattered signal on scattering centre p and B_p its amplitude. According to the radar range equation (4), and neglecting for the moment the influence of the ground, the p^{th} backscattered signal must have the shape of

$$h_{N,Tx}(t) \otimes h_{N,Rx}(t) \otimes \frac{dV_S(t)}{dt}, \qquad (6)$$

which, in the case of our laboratory UWB GPR, looks like a derivative of a Gaussian. Therefore, we designed a normalised mother wavelet to fit this shape:

$$h_{a_p,t_p}(t) = \frac{1}{\sqrt{a_p}} \sqrt{\frac{2}{\sqrt{p}}} \left(\frac{t - t_p}{a_p} \right) e^{-\frac{1}{2}\left(\frac{t-t_p}{a_p} \right)^2} \qquad (7)$$

The delay t_p takes deals with the two-way travelling time antennas-scattering centre p, and the scaling factor a_p partially compensates for the broadening of the reflection on the scattering centre. The coefficients B_p are found iteratively. First, The CWT of the received signal is computed (Hubbard, 1996), using (7) as mother wavelet. B_1 is found as being the maximum of the resulting CWT. To B_1 correspond a scale factor a_1 and a delay t_1. Afterwards $B_1 h_{a_1,t_1}(t)$ is subtracted from the received signal. This process is iterated to generate as many coefficients as needed to accurately represent the original received signal. Fig. 7 shows the result of this method on an A-scan, corresponding to a PMN mine in loam at a depth of 5 cm.

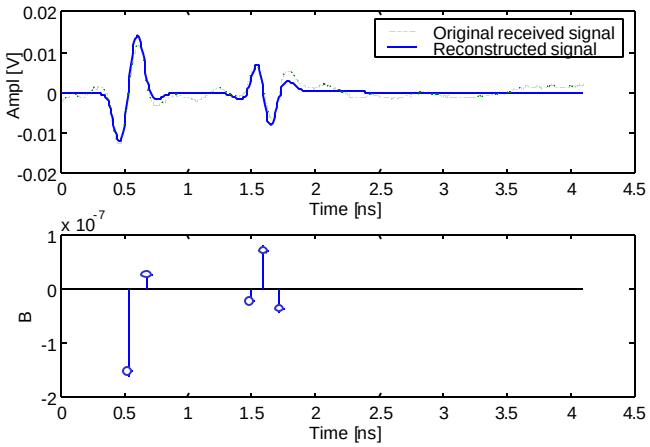

Fig. 7: Top: Approximation of A-scan as a sum of wavelets.
Bottom: Coefficients B_p of the scattering centres.

The method can also be used to reduce the amount of data for further processing. It is seen that in most of the cases an A-scan is accurately represented by a sum of 5 wavelets. Each wavelet is characterised by one triplet (B_p, t_p, a_p). This data reduction becomes important for C-scans. Fig. 8 shows a 3D representation of a PMN mine at 5 cm of depth, by representing only the scattering centres.

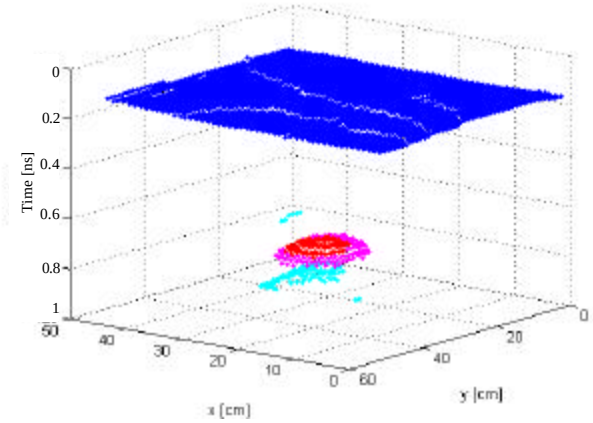

Fig. 8: 3D representation of scattering centres

RESULTS

The laboratory UWB GPR system was built to study the advantages and shortcomings of UWB systems. As a main shortcoming we already mentioned the limited range performance in wet soils. As an advantage, we expect a better depth resolution and additional information on the targets due to the larger bandwidth. Therefore some indoor tests were performed. Fig. 9 shows the raw data of a B-scan of an Italian VS/50 AP mine buried at a depth of 2 cm. It can be seen that without any signal processing, the mine can easily be distinguished from the air-ground interface.

We also tried some signal-processing techniques on A-scans, essentially based on Prony methods and on time-frequency analysis, but without much success. This is probably due to the low Q factor of the targets. None of these methods seems to be robust enough to be used for classification purposes. We therefore will orient our work in the future on B-scans and C-scans.

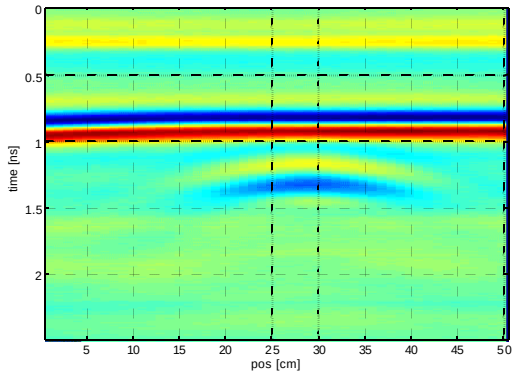

Fig. 9: B-scan of VS/50 AP mine at 2 cm depth

CONCLUSIONS

In our research on the detection and classification of plastic AP mines by means of UWB GPRs, we built a relatively simple UWB system. The main effort was put in the development of the UWB antennas, that can be used off-ground. Indoor tests revealed the capability of detecting shallow buried mines. When mines are buried deeper and the soil has a high attenuation the detection becomes almost impossible. Because of the low Q factor of the targets it is hard to extract robust features out of the A-scan, even for an UWB system. We therefore will orient our work in the future on B-scans and C-scans.

Disposing of an accurate time-domain model of the system turns out to be essential for predicting system performances and for tuning signal processing algorithms. The modelling is done by considering the system as a cascade of linear responses. An important part in this cascade is the modelling of the antennas by their normalised impulse response. The advantage of using the normalised IR is that the time-domain antenna equations become very simple and accurate to use. We developed the radar range equation directly in the time-domain. The range performance of the UWB GPR could thereby be expressed as a function of minimal detectable peak amplitude of our receiver and not in terms of a frequency depending signal power as in the standard radar range equation. It is seen that the range performance decreases dramatically with moisture. To enhance the range performance, another receiver and more instantaneous power in the impulse is needed. The time-domain model is also used to optimise the antennas offset angle. The optimal offset angle is the one that focuses the antennas on the target. In this paper we also presented a processing technique for extracting the scattering centres from the backscattered signal, by decomposing this signal into a linear combination of wavelets. The method is robust to noise and takes into account the dispersive behaviour of the ground. The method can also be used to reduce the amount of data for further processing.

REFERENCES

Daniels D.J., 1996. *Surface Penetrating Radar*, IEE, London, UK.

Farr, E.G., Baum, C.E., 1998. Time Domain Characterization of Antennas with TEM Feeds, Sensor and Simulation Notes , note 426, Air Force Research Laboratory, USA.

Hubbard, B.B., 1996. *The world according to wavelets,* A K Peters, Ltd., MA, USA, 1996.

Rumsey,V., 1966. *Frequency independent antennas,* Academic Press Inc, New York, USA.

Scheers, B., Piette, M., Vander Vorst, A., 2000a. Development of Dielectric-Filled TEM Horn Antennas for UWB GPR, submitted to *IEEE AP-2000 conference*, Switzerland, April 2000.

Scheers, B., Acheroy, M., Vander Vorst, A., 2000b. Time Domain Simulation and Characterisation of TEM Horns Using Normalised Impulse Response, submitted to *IEE Proceedings - Microwaves, Antennas and Propagation.*

Trintinalia, L.C., Ling, H., 1997. Feature extraction from elctromagnetic backscattered data using joint time-frequency processing, *Ultra-Wideband, Short-Pulse Electromagnetics 3*, Plenum Press, New York, 1997.